

THE FIRST GEOLOGICAL MAP OF THE HOKUSAI QUADRANGLE (H05) OF MERCURY. J. Wright¹, D. A. Rothery¹, M. R. Balme¹ and S. J. Conway², ¹School of Physical Sciences, The Open University, Milton Keynes, MK7 6AA, UK (jack.wright@open.ac.uk), ²CNRS UMR 6112, Laboratoire de Planétologie et Géodynamique, Université de Nantes, France.

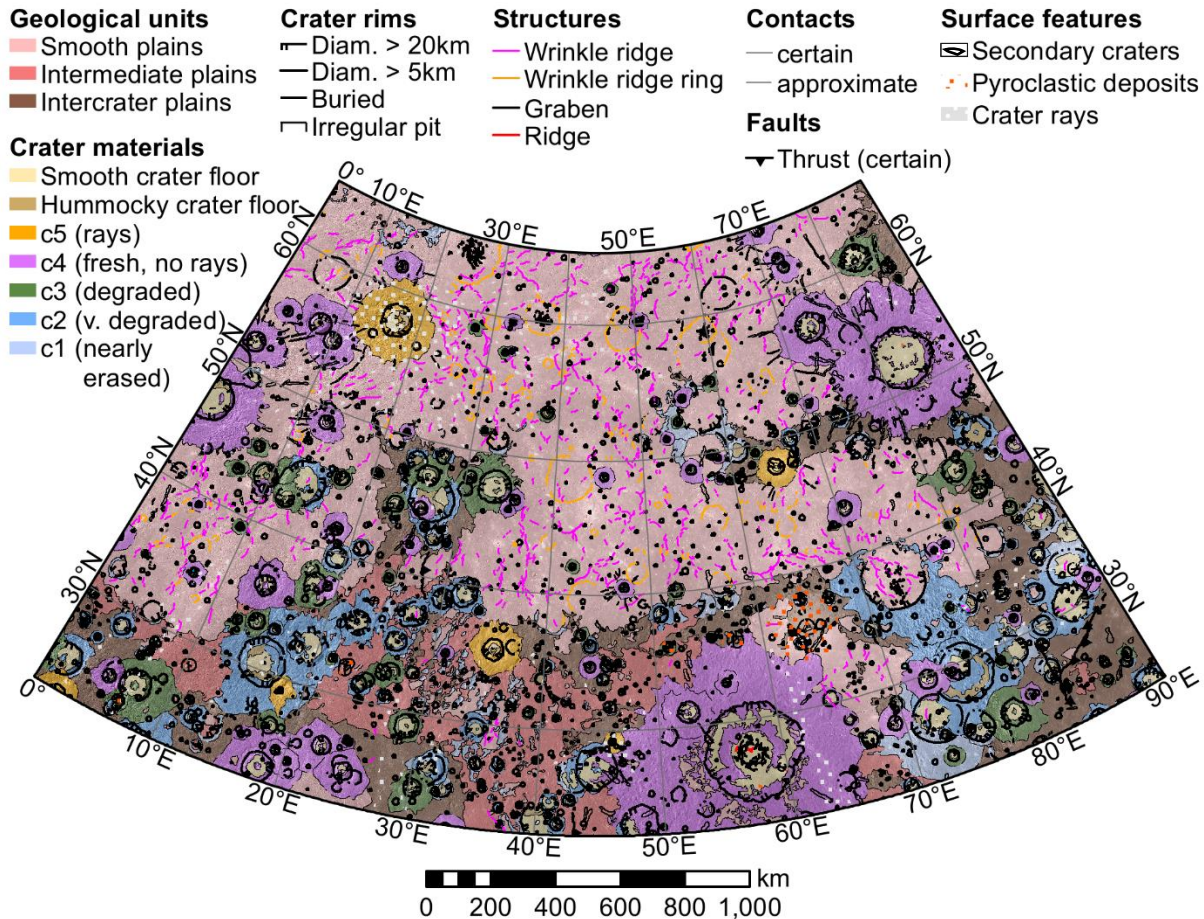


Fig. 1. Final H05 linework shown with five crater degradation classes [1]. The remaining symbology is based on that of the other published MESSENGER-era quadrangle geological maps of Mercury [2,3,4].

Introduction: Data from the MESSENGER mission are being used to create quadrangle geological maps of Mercury [2–7] in preparation for the Bepi-Colombo mission [8,9]. Here, we present our final map of the Hokusai quadrangle (H05), which has been produced as part of this international effort (Fig. 1).

Data and Methods: H05 (mid-northern latitudes; 0–90°E, 22.5–66°N) has been mapped in a Lambert Conformal Conic projection of a 2440 km radius sphere. Linework was digitized at the 1:400k scale, for publication at 1:3M scale, in accordance with USGS recommendations and the published MESSENGER-era quadrangle geological maps [2,3,4].

Geological boundaries were mainly digitized from the ~166 m/pixel MESSENGER monochrome basemap tiles for H05 [10], with additional insights provided by

monochrome mosaics with high- and low-incidence illumination from both east and west [10], enhanced color mosaics [11], and topography [12,13,14].

Mariner 10-era quadrangle mappers employed crater degradation schemes with five classes [e.g. 15]. From this, a morphostratigraphy was constructed. A similar 5-class scheme was used (craters >40 km across) during the production of the global geological map of Mercury [16]. However, MESSENGER-era quadrangle mappers found instances of small, degraded craters superposing relatively fresh, larger craters when attempting to use a 5-class scheme for craters >20 km across [2]. To avoid this, they classified craters into three classes [2]. A coherent morphostratigraphy, where superposing craters are always in a less degraded state was made, at the cost of local temporal resolution.

For H05, impact crater (>20 km across) materials were simultaneously classified according to the 3-class [2,3,4] and 5-class [1,16] degradation schemes to test if a higher resolution morphostratigraphy is viable in H05.

Mapped Units and Features:

Smooth plains. The most widespread plains unit in H05. Low density of superposing craters. Mostly Borealis Planitia (volcanic; [17]), with smaller patches perched on impact ejecta (impact melt).

Intercrater plains. Most likely cratered volcanic plains incorporating degraded impact ejecta [18].

Intermediate plains. An important plains unit within H05. Characterized by rough, locally high-standing terrain with intervening networks of low-lying material approaching the crater density of smooth plains. Similar surface textures are observed in H10 and H14 [5,6]. Embays intercrater plains. Interpreted as incomplete inundation of cratered plains by lava, as observed elsewhere on Mercury [19]. This interpretation is corroborated by candidate source vents within intermediate plains. Stratigraphic relationship with smooth plains uncertain, but they most likely formed during the same epoch.

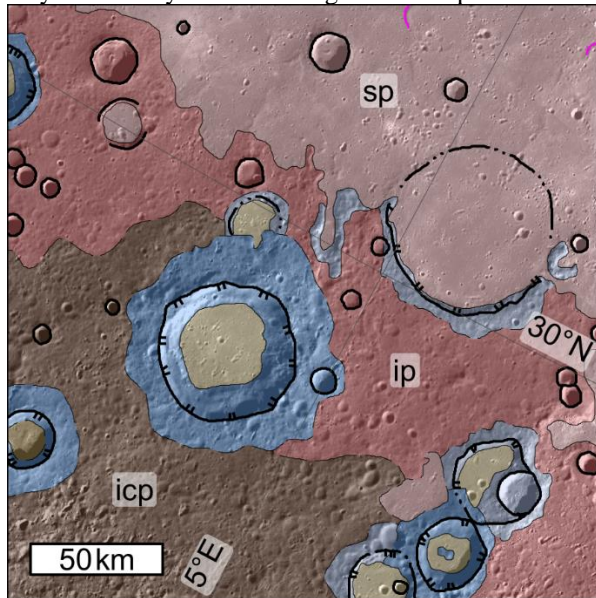


Fig. 2. Comparison of smooth plains (sp), intercrater plains (icp), and intermediate plains (ip) in H05.

Faculae. Bright, spectrally red, surficial deposits with diffuse outlines. Some contain central, irregular, rimless depressions (10s km across; e.g. in Nathair Facula), whereas others contain numerous, smaller distributed pits (e.g. Suge Facula). Ornamented so that apparent underlying geology is also rendered. Most volcanic pits on Mercury are located within impact craters that probably facilitated eruptions [20]. Prominent pits with H05's Nathair and Neidr Faculae are not in craters; their formation might instead have been facilitated by extension external to loading from Borealis Planitia [21].

Rays. Bright, spectrally blue, surficial deposits occurring as haloes around, and streaks radiating from, fresh impact craters. Rays from Hokusai crater extend over much of H05 and the rest of Mercury, making them potentially useful as a stratigraphic marker.

Tectonic features. H05 contains abundant wrinkle ridges in its smooth plains that appear to have formed due to global contraction [22]. These often form rings indicating buried ('ghost') impact craters. Ghost craters often contain graben networks [23]. Smooth plains within Rachmaninoff also contain grabens and ridges that probably formed by thermal contraction lavas [24].

Crater classification: For craters >20 km across, no instance of more-degraded craters superposing less-degraded craters was observed in the 5-class scheme. As such, a higher temporal resolution morphostratigraphy is available for H05 than the published MESSENGER-era quadrangle maps [2,3,4]. This is due to the high proportion of smooth plains in H05, which means this quadrangle has relatively few degraded craters. We recommend that future quadrangle mappers also test the 5-class scheme, and default to the 3-class scheme only if they observe degradation contradicting stratigraphy.

Future Work: This map will be submitted to the Journal of Maps shortly. We will meet with the mappers of the adjacent quadrangles with published maps [2,3] to fix the contacts at the boundaries between our maps.

Acknowledgements: This is a contribution to Planmap (EU Horizon 2020 grant 776276).

References: [1] Kinczyk M. J. et al. (2016) *LPS XLVII*, #1573. [2] Galluzzi V. et al. (2016) *J. Maps*, 12, 227–238. [3] Mancinelli P. et al. (2016) *J. Maps*, 12, 190–202. [4] Guzzetta L. et al. (2017) *J. Maps*, 13, 227–238. [5] Malliband C. C. et al. (2019) *LPS L*, #1807. [6] Pegg D. L. et al. (2019) *LPS L*, #1271. [7] Galluzzi V. et al. (2018) *Mercury*, #6075. [8] Benkhoff J. et al. (2010) *Planet. Space Sci.*, 58, 2–20. [9] Rothery D. A. et al. (2010) *Planet. Space Sci.*, 58, 21–39. [10] Chabot N. L. et al. (2016) *LPS XLVII*, #1256. [11] Denevi B. W. (2016) *LPS XLVII*, #1264. [12] Zuber M. T. (2012) *Science*, 336, 217–220. [13] Becker K. J. (2016) *LPS XLVII*, #2959. [14] Stark A. et al (2017) *LPS XLVIII*, #2287. [15] Strom R. G. et al. (1990) USGS Miscellaneous Investigations Series, Map I–2015. [16] Kinczyk M. J. (2018) *Mercury*, #6123. [17] Ostrach L. R. et al (2015) *Icarus*, 250, 602–622. [18] Whitten J. L. et al. (2014) *Icarus*, 241, 97–113. [19] Byrne P. K. et al. (2013) *J. Geophys. Res. Planets*, 118, 1303–1322. [20] Jozwiak L. M. et al. (2018) *Icarus*, 302, 191–212. [21] McGovern P. J. and Litherland M. M. (2011) *LPS XLII*, #2587. [22] Crane K. T. and Klimczak C. (2019) *Icarus*, 317, 66–80. [23] Freed A. M. et al. (2012) *J. Geophys. Res.*, 117, E00L06. [24] Blair D. M. et al. (2013) *J. Geophys. Res. Planets*, 118, 47–58.